A field expansions method for scattering by periodic multilayered media

Alison Malcolm
Department of Earth, Atmospheric, and Planetary Sciences, Massachusetts Institute of Technology
David P. Nicholls
Department of Mathematics, Statistics, and Computer Science, University of Illinois at Chicago

Abstract

The interaction of acoustic and electromagnetic waves with periodic structures plays an important role in a wide range of problems of scientific and technological interest. This contribution focuses upon the robust and high-order numerical simulation of a model for the interaction of pressure waves generated within the earth incident upon layers of sediment near the surface. Herein is described a Boundary Perturbation Method for the numerical simulation of scattering returns from irregularly shaped periodic layered media. The method requires only the discretization of the layer interfaces (so that the number of unknowns is an order of magnitude smaller than Finite Difference and Finite Element simulations), while it avoids not only the need for specialized quadrature rules but also the dense linear systems characteristic of Boundary Integral/Element Methods. The approach is a generalization to multiple layers of Bruno & Reitich's "Method of Field Expansions" for dielectric structures with two layers. By simply considering the entire structure simultaneously, rather than solving in individual layers separately, the full field can be recovered in time proportional to the number of interfaces. As with the original Field Expansions method, this approach is extremely efficient and spectrally accurate.

1 Introduction

The interaction of acoustic and electromagnetic waves with periodic structures plays an important role in a wide range of problems of scientific and technological interest. From grating couplers to nanostructures to remote sensing, the ability to simulate in a robust and accurate way the fields generated by such structures is of crucial importance to researchers from many disciplines. In this contribution we focus upon the robust and high–order numerical simulation of a model for the interaction of pressure waves generated within the earth incident upon layers of sediment near the surface. While we focus on the simplified model of acoustic waves in a two–dimensional structure, the issues we address are the largely the same as those which arise in a three–dimensional simulation of the full equations of elasticity.

This problem is motivated jointly by the recent increased interest in oil exploration in mountainous regions, and the rash of recent large earthquakes, which tend to occur in regions with significant topography. Simulating the seismic wavefield accurately in such regions is key for both imaging (e.g. through waveform inversion, see Virieux[31] for a recent review and Bleibinhaus[2] for a specific discussion of topography in such algorithms), and hazard assessment [10, 29]. A wide array of numerical algorithms have been devised in the past fifty years for the simulation of precisely the problem we consider. The classical Finite Difference (FDM) [22, 28], Finite Element (FEM) [33, 13], and Spectral Element (SEM) [14, 15] methods are available but suffer from the fact that they discretize the full volume of the model which not only introduces a huge number of degrees of freedom, but also raises the difficult question of appropriately specifying a far–field boundary condition explicitly. Furthermore, the Finite Difference method, while simple to devise and implement is not well–suited to the complex geometries of general layered media. A compelling alternative are *surface* integral methods [30, 3] (e.g. Boundary Integral Methods—BIM—or Boundary Element Methods—BEM) which only require a discretization of the layer *interfaces* (rather than the whole structure) and which, due to the choice of the Green's function, enforce the far–field boundary condition exactly. While these methods can deliver high–accuracy simulations with greatly reduced operation counts, there are several difficulties which need to be addressed. First, high–order simulations can only be realized with specially designed quadrature rules which respect the singularities in the Green's function (and its derivative, in certain formulations). Additionally, BIM/BEM typically give rise to dense linear systems to be solved which require carefully designed preconditioned iterative methods (with accelerated matrix–vector products, e.g., by the Fast–Multipole Method [12]) for configurations of engineering interest.

In this work we describe a novel Boundary Perturbation Method (BPM) for the numerical simulation of scattering returns from irregularly shaped periodic layered media. Like BIM/BEM, the method requires only

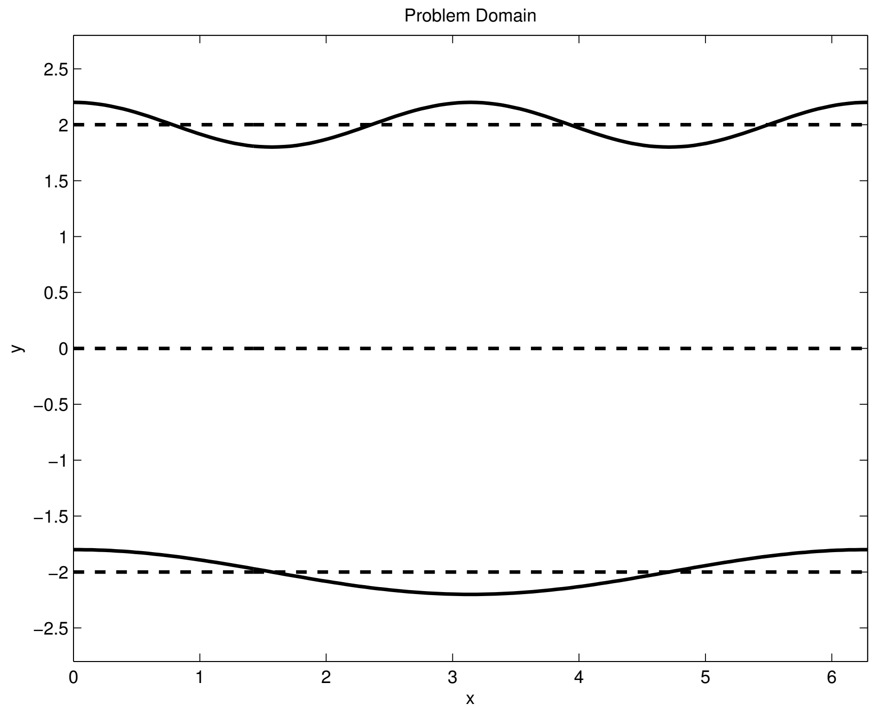

Figure 1: Plot of problem domain with layer boundaries in solid lines, and mid–levels in dashed lines. Here $\bar{g} = 2$, $\bar{h} = -2$, $g(x) = 0.2\cos(x)$, $h(x) = 0.2\cos(2x)$, and $\bar{m} = 0$.

the discretization of the layer interfaces (so that the number of unknowns is an order of magnitude smaller than FDM, FEM, and SEM simulations), while it avoids not only the need for specialized quadrature rules but also the dense linear systems characteristic of BIM/BEM. Our approach is a generalization of the "Method of Field Expansions" (FE) described by Bruno & Reitich [4, 5, 6, 7] for dielectric structures with two layers (denoted there the "Method of Variation of Boundaries"). This method is similar in spirit to the "Method of Operator Expansions" (OE) of Milder [16, 17, 20, 21, 19, 18] and the "Transformed Field Expansions" (TFE) approach of the author and Reitich [23, 24, 25, 26] and these approaches could also be extended in the way we describe here, however, we save this for future work as the FE approach is the simplest to implement. The FE method was generalized by Hesthaven and collaborators to the case of grating couplers and layered media [8, 9, 32], precisely the problem we consider here, though we have found their method to be highly inefficient. As we discuss at the end of § 3.2, their approach relies on the iterative solution of the problem from one layer to the next with the two–layer solver of Bruno & Reitich [5], applied sequentially to each pair of layers. After a *great* number of iterations, this method will eventually converge to the fully scattered field at enormous computational cost. We have found that by simply considering the *entire* structure (more specifically the full set of *interfaces*), the full field can be recovered simultaneously in time proportional to the number of interfaces. As with the FE method as it was originally designed by Bruno & Reitich, our new approach is spectrally accurate (i.e., convergence rates faster than any polynomial order) due to both the analyticity of the scattered fields with respect to boundary perturbation, and the optimal choice of spatial basis functions which arise naturally from the FE methodology.

The organization of the paper is as follows: In § 2 we recall the governing equations of acoustic scattering in a triply layered medium, and in § 2.1 and § 2.2 we describe our FE approach for such media with trivial (flat) and non–trivial (perturbed) layering structure, respectively. In § 3, § 3.1, and § 3.2 we repeat these considerations for the general $(M + 1)$–layer case. In § 4 we display results of numerical simulations for three– and five–layer structures to demonstrate the accuracy, efficiency, reliability, and flexibility of our new numerical algorithm.

2 Field Expansions: Three Layers

For ease of exposition we begin by describing the case of a triply layered material in two dimensions. In each of the layers the scattered pressure satisfies the Helmholtz equation with continuity conditions at the upper interface, illumination conditions at the lower interface, and outgoing wave conditions at positive and negative infinity. More precisely, we define the domains

$$S_u := \{(x,y) \mid y > \bar{g} + g(x)\}$$
$$S_v := \left\{(x,y) \mid \bar{h} + h(x) < y < \bar{g} + g(x)\right\}$$
$$S_w := \left\{(x,y) \mid y < \bar{h} + h(x)\right\},$$

with (upward pointing) normals

$$N_g := (-\partial_x g, 1)^T, \quad N_h := (-\partial_x h, 1)^T;$$

see Figure 1.

In each of these domains is a constant–density acoustic medium with velocity c_j $(j = u, v, w)$; we assume that plane–wave radiation is incident upon the structure from below:

$$\tilde{w}(x,y,t) = e^{-i\omega t} e^{i(\alpha x + \beta y)} =: e^{-i\omega t} w_i(x,y). \tag{1}$$

With these specifications we can define in each layer the parameter $k_j = \omega / c_j$ which characterizes both the properties of the material and the frequency of radiation in the structure. If the reduced scattered fields in S_u, S_v, and S_w are respectively denoted $\{u, v, w\} = \{u(x,y), v(x,y), w(x,y)\}$ then the system of partial differential equations to be solved are:

$$\Delta u + k_u^2 u = 0 \qquad y > \bar{g} + g(x) \tag{2a}$$
$$\text{OWC}[u] = 0 \qquad y \to \infty \tag{2b}$$
$$\Delta v + k_v^2 v = 0 \qquad \bar{h} + h(x) < y < \bar{g} + g(x) \tag{2c}$$
$$u - v = 0, \quad \partial_{N_g}(u - v) = 0 \qquad y = \bar{g} + g(x) \tag{2d}$$
$$\Delta w + k_w^2 w = 0 \qquad y < \bar{h} + h(x) \tag{2e}$$
$$\text{OWC}[w] = 0 \qquad y \to -\infty \tag{2f}$$
$$v - w = \xi, \quad \partial_{N_h}(v - w) = \psi \qquad y = \bar{h} + h(x), \tag{2g}$$

where

$$\xi(x) := -w_i(x, \bar{h} + h(x)), \quad \psi(x) := -\left[\partial_{N_h} w_i(x,y)\right]_{y = \bar{h} + h(x)}. \tag{2h}$$

In these equations OWC denotes the "Outgoing Wave Condition" [27] and states that the field must be upward and downward propagating in S_u and S_w, respectively.

The solutions of the Helmholtz equations—(2a), (2c) & (2e)—and the Outgoing Wave Conditions—(2b) & (2f)— are given by [27]

$$u(x,y) = \sum_{p=-\infty}^{\infty} a_p \exp(i(\alpha_p x + \beta_{u,p}(y - \bar{g}))) \tag{3a}$$

$$v(x,y) = \sum_{p=-\infty}^{\infty} b_p \exp(i(\alpha_p x - \beta_{v,p}(y - \bar{m}))) + \sum_{p=-\infty}^{\infty} c_p \exp(i(\alpha_p x + \beta_{v,p}(y - \bar{m}))) \tag{3b}$$

$$w(x,y) = \sum_{p=-\infty}^{\infty} d_p \exp(i(\alpha_p x - \beta_{w,p}(y - \bar{h}))), \tag{3c}$$

where $\bar{m} = (\bar{g} + \bar{h})/2$, provided that (x, y) are *outside* the grooves, i.e.

$$(x, y) \in \{y > \bar{g} + |g|_{L^\infty}\} \cup \{\bar{h} + |h|_{L^\infty} < y < \bar{g} - |g|_{L^\infty}\} \cup \{y < \bar{h} - |h|_{L^\infty}\}.$$

In these equations

$$\alpha_p := \alpha + (2\pi/d)p, \quad \beta_p := \begin{cases} \sqrt{k_j^2 - \alpha_p^2} & \alpha_p^2 < k_j^2 \\ i\sqrt{\alpha_p^2 - k_j^2} & \alpha_p^2 > k_j^2 \end{cases}, \tag{4}$$

$j = u, v, w$ and d is the period of the structure. The boundary conditions—(2d) & (2g)— determine the coefficients $\{a_p, b_p, c_p, d_p\}$.

2.1 Trivial Interfaces

In the case where the interfaces are flat (i.e., $g = h \equiv 0$) then the equations for $\vec{z}_p := (a_p, b_p, c_p, d_p)^T$ become quite straightforward. In light of (3), (2d) & (2g) mandate that

$$0 = \sum_{p=-\infty}^{\infty} \exp(i\alpha_p x) \{a_p - b_p \exp(-i\beta_{v,p}(\bar{g} - \bar{m})) - c_p \exp(i\beta_{v,p}(\bar{g} - \bar{m}))\} \tag{5a}$$

$$0 = \sum_{p=-\infty}^{\infty} \exp(i\alpha_p x) \{(i\beta_{u,p})a_p - (-i\beta_{v,p})b_p \exp(-i\beta_{v,p}(\bar{g} - \bar{m})) - (i\beta_{v,p})c_p \exp(i\beta_{v,p}(\bar{g} - \bar{m}))\} \tag{5b}$$

$$\xi(x) = \sum_{p=-\infty}^{\infty} \exp(i\alpha_p x) \left\{b_p \exp(-i\beta_{v,p}(\bar{h} - \bar{m})) + c_p \exp(i\beta_{v,p}(\bar{h} - \bar{m})) - d_p\right\} \tag{5c}$$

$$\psi(x) = \sum_{p=-\infty}^{\infty} \exp(i\alpha_p x) \left\{(-i\beta_{v,p})b_p \exp(-i\beta_{v,p}(\bar{h} - \bar{m})) + (i\beta_{v,p})c_p \exp(i\beta_{v,p}(\bar{h} - \bar{m})) - (-i\beta_{w,p})d_p\right\}. \tag{5d}$$

Alternatively, if we view the coefficients $\{a_p, b_p, c_p, d_p\}$ as defining the (generalized) Fourier coefficients of functions $\{a(x), b(x), c(x), d(x)\}$ via

$$(a(x), b(x), c(x), d(x))^T := \sum_{p=-\infty}^{\infty} (a_p, b_p, c_p, d_p)^T \exp(i\alpha_p x),$$

then (5) states that

$$0 = a(x) - D_g[b(x)] - U_g[c(x)] \tag{6a}$$

$$0 = B_u[a(x)] + B_v[D_g[b(x)]] - B_v[U_g[c(x)]] \tag{6b}$$

$$\xi(x) = D_h[b(x)] + U_h[c(x)] - d(x) \tag{6c}$$

$$\psi(x) = -B_v[D_h[b(x)]] + B_v[U_h[c(x)]] + B_w[d(x)], \tag{6d}$$

where we have defined the order–zero Fourier multipliers

$$U_g[\zeta(x)] := \sum_{p=-\infty}^{\infty} \exp(i\beta_{v,p}(\bar{g} - \bar{m}))\hat{\zeta}_p \tag{7a}$$

$$D_g[\zeta(x)] := \sum_{p=-\infty}^{\infty} \exp(-i\beta_{v,p}(\bar{g} - \bar{m}))\hat{\zeta}_p \tag{7b}$$

$$U_h[\zeta(x)] := \sum_{p=-\infty}^{\infty} \exp(i\beta_{v,p}(\bar{h} - \bar{m}))\hat{\zeta}_p \tag{7c}$$

$$D_h[\zeta(x)] := \sum_{p=-\infty}^{\infty} \exp(-i\beta_{v,p}(\bar{h} - \bar{m}))\hat{\zeta}_p \tag{7d}$$

and the order–one Fourier multipliers

$$B_u[\zeta(x)] := \sum_{p=-\infty}^{\infty} (i\beta_{u,p})\hat{\zeta}_p \tag{8a}$$

$$B_v[\zeta(x)] := \sum_{p=-\infty}^{\infty} (i\beta_{v,p})\hat{\zeta}_p \tag{8b}$$

$$B_w[\zeta(x)] := \sum_{p=-\infty}^{\infty} (i\beta_{w,p})\hat{\zeta}_p. \tag{8c}$$

Upon expansion of $\xi(x)$ and $\psi(x)$ in (generalized) Fourier series

$$\xi(x) = \sum_{p=-\infty}^{\infty} \hat{\xi}_p \exp(i\alpha_p x), \quad \psi(x) = \sum_{p=-\infty}^{\infty} \hat{\psi}_p \exp(i\alpha_p x),$$

we can write (5) (equivalently (6)) “wavenumber–by–wavenumber” as

$$\mathcal{A}_p \vec{z}_p = \vec{r}_p \tag{9}$$

where

$$\mathcal{A}_p := \begin{pmatrix} 1 & -\exp(-i\beta_{v,p}(\bar{g} - \bar{m})) & -\exp(i\beta_{v,p}(\bar{g} - \bar{m})) & 0 \\ (i\beta_{u,p}) & (i\beta_{v,p})\exp(-i\beta_{v,p}(\bar{g} - \bar{m})) & -(i\beta_{v,p})\exp(i\beta_{v,p}(\bar{g} - \bar{m})) & 0 \\ 0 & \exp(-i\beta_{v,p}(\bar{h} - \bar{m})) & \exp(i\beta_{v,p}(\bar{h} - \bar{m})) & -1 \\ 0 & -(i\beta_{v,p})\exp(-i\beta_{v,p}(\bar{h} - \bar{m})) & (i\beta_{v,p})\exp(i\beta_{v,p}(\bar{h} - \bar{m})) & (i\beta_{w,p}) \end{pmatrix}$$

and

$$\vec{r}_p := (0, 0, \hat{\xi}_p, \hat{\psi}_p)^T.$$

2.2 Non–Trivial Interfaces

To deal with non–trivial interfaces we once again appeal to the representations (3) which satisfy the Helmholtz equations and Outgoing Wave Conditions. As before, the boundary conditions (2d) & (2g) determine the coefficients $\vec{z}_p = (a_p, b_p, c_p, d_p)^T$, however, these conditions must be understood as g– and h–dependent equations. For instance, we may enforce (6) where the operators U_g, D_g, U_h, and D_h must now be generalized to:

$$U_g(g)[\zeta(x)] := \sum_{p=-\infty}^{\infty} \exp(i\beta_{v,p}(\bar{g}+g-\bar{m}))\hat{\zeta}_p \tag{10a}$$

$$D_g(g)[\zeta(x)] := \sum_{p=-\infty}^{\infty} \exp(-i\beta_{v,p}(\bar{g}+g-\bar{m}))\hat{\zeta}_p \tag{10b}$$

$$U_h(h)[\zeta(x)] := \sum_{p=-\infty}^{\infty} \exp(i\beta_{v,p}(\bar{h}+h-\bar{m}))\hat{\zeta}_p \tag{10c}$$

$$D_h(h)[\zeta(x)] := \sum_{p=-\infty}^{\infty} \exp(-i\beta_{v,p}(\bar{h}+h-\bar{m}))\hat{\zeta}_p. \tag{10d}$$

The Method of Field Expansions (FE) [5] as applied to (6) supposes that if the interfaces are *small* perturbations of the flat interface case, $g(x) = \varepsilon f(x)$ and $h(x) = \varepsilon s(x)$, then the fields $\{u, v, w\} = \{u(x, y; \varepsilon), v(x, y; \varepsilon), w(x, y; \varepsilon)$ will depend *analytically* upon ε, allowing the Taylor expansion about $\varepsilon = 0$

$$\begin{aligned}
u(x,y;\varepsilon) &= \sum_{p=-\infty}^{\infty} a_p(\varepsilon)\exp(i(\alpha_p x + \beta_{u,p}(y-\bar{g}))) = \sum_{p=-\infty}^{\infty}\sum_{n=0}^{\infty} a_{p,n}\varepsilon^n \exp(i(\alpha_p x + \beta_{u,p}(y-\bar{g}))) \\
v(x,y;\varepsilon) &= \sum_{p=-\infty}^{\infty} b_p(\varepsilon)\exp(i(\alpha_p x - \beta_{v,p}(y-\bar{m}))) + \sum_{p=-\infty}^{\infty} c_p(\varepsilon)\exp(i(\alpha_p x + \beta_{v,p}(y-\bar{m}))) \\
&= \sum_{p=-\infty}^{\infty}\sum_{n=0}^{\infty} b_{p,n}\varepsilon^n \exp(i(\alpha_p x - \beta_{v,p}(y-\bar{m}))) + \sum_{p=-\infty}^{\infty}\sum_{n=0}^{\infty} c_{p,n}\varepsilon^n \exp(i(\alpha_p x + \beta_{v,p}(y-\bar{m})) \\
w(x,y;\varepsilon) &= \sum_{p=-\infty}^{\infty} d_p(\varepsilon)\exp(i(\alpha_p x - \beta_{w,p}(y-\bar{h}))) = \sum_{p=-\infty}^{\infty}\sum_{n=0}^{\infty} d_{p,n}\varepsilon^n \exp(i(\alpha_p x - \beta_{w,p}(y-\bar{h}))).
\end{aligned}$$

To determine the $\vec{z}_{p,n} := (a_{p,n}, b_{p,n}, c_{p,n}, d_{p,n})^T$ we consider the generalization of equation (6)

$$0 = a(x;\varepsilon) - D_g(\varepsilon f)[b(x;\varepsilon)] - U_g(\varepsilon f)[c(x;\varepsilon)] \tag{11a}$$

$$0 = B_u[a(x;\varepsilon)] + B_v[D_g(\varepsilon f)[b(x;\varepsilon)]] - B_v[U_g(\varepsilon f)[c(x;\varepsilon)]] \tag{11b}$$

$$\xi(x) = D_h(\varepsilon s)[b(x;\varepsilon)] + U_h(\varepsilon s)[c(x;\varepsilon)] - d(x;\varepsilon) \tag{11c}$$

$$\psi(x) = -B_v[D_h(\varepsilon s)[b(x;\varepsilon)]] + B_v[U_h(\varepsilon s)[c(x;\varepsilon)]] + B_w[d(x;\varepsilon)]. \tag{11d}$$

Expanding the functions and operators in Taylor series result in

$$\begin{aligned}
0 &= \sum_{n=0}^{\infty}\varepsilon^n\left(a_n(x) - \sum_{l=0}^{n} D_{g,n-l}(f)[b_l(x)] - \sum_{l=0}^{n} U_{g,n-l}(f)[c_l(x)]\right) \\
0 &= \sum_{n=0}^{\infty}\varepsilon^n\left(B_u[a_n(x)] + \sum_{l=0}^{n} B_v[D_{g,n-l}(f)[b_l(x)]] - \sum_{l=0}^{n} B_v[U_{g,n-l}(f)[c_l(x)]]\right) \\
\xi(x) &= \sum_{n=0}^{\infty}\varepsilon^n\left(\sum_{l=0}^{n} D_{h,n-l}(s)[b_l(x)] + \sum_{l=0}^{n} U_{h,n-l}(s)[c_l(x)] - d_n(x)\right) \\
\psi(x) &= \sum_{n=0}^{\infty}\varepsilon^n\left(-\sum_{l=0}^{n} B_v[D_{h,n-l}(s)[b_l(x)]] + \sum_{l=0}^{n} B_v[U_{h,n-l}(s)[c_l(x)]] + B_w[d_n(x)]\right).
\end{aligned}$$

For clarity of exposition we note that our notation in these and subsequent formulas is

$$a(x;\varepsilon) = \sum_{n=0}^{\infty}\sum_{p=-\infty}^{\infty} a_{p,n}e^{i\alpha_p x}\varepsilon^n = \sum_{n=0}^{\infty} a_n(x)\varepsilon^n = \sum_{p=-\infty}^{\infty} a_p(\varepsilon)e^{i\alpha_p x},$$

and similarly for b, c, and d; note that, of course, $a_n(x) \neq a_p(\varepsilon)$.

It is not difficult to see that

$$U_{g,0} = U_g(0), \quad D_{g,0} = D_g(0), \quad U_{h,0} = U_h(0), \quad D_{h,0} = D_h(0),$$

so that at order $n = 0$ this amounts to precisely (6) or, at each wave–number p,

$$\mathcal{A}_p \vec{z}_{p,0} = \vec{r}_p \tag{12}$$

c.f. (9). For $n > 0$ we must solve

$$\begin{aligned}
a_n(x) - D_{g,0}[b_n(x)] - U_{g,0}[c_n(x)] &= \sum_{l=0}^{n-1} D_{g,n-l}(f)[b_l(x)] + \sum_{l=0}^{n-1} U_{g,n-l}(f)[c_l(x)] \\
B_u[a_n(x)] + B_v[D_{g,0}[b_n(x)]] - B_v[U_{g,0}[c_n(x)]] &= -\sum_{l=0}^{n-1} B_v[D_{g,n-l}(f)[b_l(x)]] \\
&\quad + \sum_{l=0}^{n-1} B_v[U_{g,n-l}(f)[c_l(x)]] \\
D_{h,0}[b_n(x)] + U_{h,0}[c_n(x)] - d_n(x) &= -\sum_{l=0}^{n-1} D_{h,n-l}(s)[b_l(x)] - \sum_{l=0}^{n-1} U_{h,n-l}(s)[c_l(x)] \\
-B_v[D_{h,0}[b_n(x)]] + B_v[U_{h,0}[c_n(x)]] + B_w[d_n(x)] &= \sum_{l=0}^{n-1} B_v[D_{h,n-l}(s)[b_l(x)]] \\
&\quad - \sum_{l=0}^{n} B_v[U_{h,n-l}(s)[c_l(x)]],
\end{aligned}$$

which, for each wave–number p, amounts to

$$\mathcal{A}_p \vec{z}_{p,n} = \vec{R}_{p,n} \tag{13}$$

where $\vec{R}_{p,n}$ are the (generalized) Fourier coefficients of the right hand sides $\vec{R}_n$

$$\vec{R}_n := \sum_{l=0}^{n-1} \begin{pmatrix} D_{g,n-l}(f)[b_l(x)] + U_{g,n-l}(f)[c_l(x)] \\ -B_v[D_{g,n-l}(f)[b_l(x)]] + B_v[U_{g,n-l}(f)[c_l(x)]] \\ -D_{h,n-l}(s)[b_l(x)] - U_{h,n-l}(s)[c_l(x)] \\ B_v[D_{h,n-l}(s)[b_l(x)]] - B_v[U_{h,n-l}(s)[c_l(x)]] \end{pmatrix}.$$

We emphasize that the matrix $\mathcal{A}_p$ need be constructed and inverted only once per p to determine the entire solution. Using the definitions of U_g, D_g, U_h, and D_h, c.f. (10), we find that

$$\begin{aligned}
U_{g,n}(f)[\zeta(x)] &= \sum_{p=-\infty}^{\infty} F_n (i\beta_{v,p})^n \exp(i\beta_{v,p}(\bar{g} - \bar{m}))\hat{\zeta}_p = F_n B_v^n[U_{g,0}[\zeta]] \\
D_{g,n}(f)[\zeta(x)] &= \sum_{p=-\infty}^{\infty} F_n (-i\beta_{v,p})^n \exp(-i\beta_{v,p}(\bar{g} - \bar{m}))\hat{\zeta}_p = F_n (-B_v)^n[D_{g,0}[\zeta]] \\
U_{h,n}(s)[\zeta(x)] &= \sum_{p=-\infty}^{\infty} S_n (i\beta_{v,p})^n \exp(i\beta_{v,p}(\bar{h} - \bar{m}))\hat{\zeta}_p = S_n B_v^n[U_{h,0}[\zeta]] \\
D_{h,n}(s)[\zeta(x)] &= \sum_{p=-\infty}^{\infty} S_n (-i\beta_{v,p})^n \exp(-i\beta_{v,p}(\bar{h} - \bar{m}))\hat{\zeta}_p = S_n (-B_v)^n[D_{h,0}[\zeta]],
\end{aligned}$$

where $F_n := (f(x)^n)/n!$, $S_n := (s(x)^n)/n!$. In this way we see that

$$\vec{R}_n = \sum_{l=0}^{n-1} F_{n-l} \begin{pmatrix} F_{n-l}\left\{(-B_v)^{n-l}[D_{g,0}[b_l(x)]] + B_v^{n-l}[U_{g,0}[c_l(x)]]\right\} \\ F_{n-l}\left\{-B_v[(-B_v)^{n-l}[D_{g,0}[b_l(x)]]] + B_v[B_v^{n-l}[U_{g,0}[c_l(x)]]]\right\} \\ S_{n-l}\left\{-(-B_v)^{n-l}[D_{h,0}[b_l(x)]] - B_v^{n-l}[U_{h,0}[c_l(x)]]\right\} \\ S_{n-l}\left\{B_v[(-B_v)^{n-l}[D_{h,0}[b_l(x)]]] - B_v[B_v^{n-l}[U_{h,0}[c_l(x)]]]\right\} \end{pmatrix}.$$

3 Field Expansions: $(M+1)$ Layers

In the general $(M+1)$–layer case ($M > 1$) we consider interfaces specified at $y = a^{(m)} + g^{(m)}(x)$ for $1 \leq m \leq M$. Defining the domains

$$\begin{aligned} S^{(0)} &:= \left\{(x,y) \mid y > a^{(1)} + g^{(1)}(x)\right\} \\ S^{(m)} &:= \left\{(x,y) \mid a^{(m+1)} + g^{(m+1)}(x) < y < a^{(m)} + g^{(m)}(x)\right\}, \quad 1 \leq m \leq M-1 \\ S^{(M)} &:= \left\{(x,y) \mid y < a^{(M)} + g^{(M)}(x)\right\}, \end{aligned}$$

with normals $N^{(m)} := (-\partial_x g^{(m)}, 1)^T$, the scattered field v satisfies the system of Helmholtz equations (c.f. (2a), (2c), & (2e)):

$$\Delta v^{(m)} + (k^{(m)})^2 v^{(m)} = 0 \quad \text{in } S^{(m)}, \quad 0 \leq m \leq M,$$

where $v^{(m)}$ is v restricted to $S^{(m)}$. For incident radiation of the form (1) one has $k^{(m)} = \omega/c_m$. These must be supplemented with the general boundary conditions:

$$\left[v^{(m-1)} - v^{(m)}\right]_{y=a^{(m)}+g^{(m)}} = \xi^{(m)}, \quad 1 \leq m \leq M, \tag{14a}$$

$$\left[\partial_{N^{(m)}} v^{(m-1)} - \partial_{N^{(m)}} v^{(m)}\right]_{y=a^{(m)}+g^{(m)}} = \psi^{(m)}, \quad 1 \leq m \leq M, \tag{14b}$$

c.f. (2d) & (2g), where $\xi^{(m)} \equiv 0$, $\psi^{(m)} \equiv 0$ for $m \neq M$, for a plane-wave incident from below; we briefly discuss other incident fields in the next section. Again, the solutions of these Helmholtz problems *outside* the grooves are

$$v^{(m)}(x,y) = \sum_{p=-\infty}^{\infty} d_p^{(m)} \exp(i(\alpha_p x - \beta_p^{(m)}(y - \bar{a}^{(m)}))) + \sum_{p=-\infty}^{\infty} u_p^{(m)} \exp(i(\alpha_p x + \beta_p^{(m)}(y - \bar{a}^{(m)}))), \tag{15}$$

where the $\bar{a}^{(m)}$ are the mid–levels of each layer:

$$\bar{a}^{(0)} := a^{(1)}, \quad \bar{a}^{(m)} := \frac{1}{2}\left(a^{(m)} + a^{(m+1)}\right), \quad \bar{a}^{(M)} := a^{(M)},$$

and

$$\beta_p := \begin{cases} \sqrt{(k^{(m)})^2 - \alpha_p^2} & \alpha_p^2 < (k^{(m)})^2 \\ i\sqrt{\alpha_p^2 - (k^{(m)})^2} & \alpha_p^2 > (k^{(m)})^2 \end{cases}.$$

The OWC can be enforced by choosing $d_p^{(0)} = u_p^{(M)} \equiv 0$. To determine the other coefficients we appeal to the boundary conditions at the interfaces $y = a^{(m)} + g^{(m)}(x)$, (14).

3.1 Trivial Interfaces

For the case of flat (trivial) interfaces, i.e. $g^{(m)} \equiv 0$ for $1 \leq m \leq M$, the Dirichlet condition (14a) coupled to the representation (15) states that

$$\begin{aligned}\xi^{(m)}(x) = \sum_{p=-\infty}^{\infty} \Big\{ & d_p^{(m-1)} \exp(-i\beta_p^{(m-1)}(a^{(m)} - \bar{a}^{(m-1)})) \\ & + u_p^{(m-1)} \exp(i\beta_p^{(m-1)}(a^{(m)} - \bar{a}^{(m-1)})) \\ & - d_p^{(m)} \exp(-i\beta_p^{(m)}(a^{(m)} - \bar{a}^{(m)})) \\ & - u_p^{(m)} \exp(i\beta_p^{(m)}(a^{(m)} - \bar{a}^{(m)})) \Big\} \exp(i\alpha_p x),\end{aligned}$$

or, in operator notation,

$$\xi^{(m)} = D^{(m,m-1)} d^{(m-1)} + U^{(m,m-1)} u^{(m-1)} - D^{(m,m)} d^{(m)} - U^{(m,m)} u^{(m)} \tag{16}$$

(recall that $d^{(0)} = u^{(M)} \equiv 0$), c.f. (6), where we have defined the order–zero Fourier multipliers:

$$\begin{aligned} D^{(m,l)}[\zeta] &:= \sum_{p=-\infty}^{\infty} \exp(-i\beta_p^{(l)}(a^{(m)} - \bar{a}^{(l)})) \hat{\zeta}_p \exp(i\alpha_p x) \\ U^{(m,l)}[\zeta] &:= \sum_{p=-\infty}^{\infty} \exp(i\beta_p^{(l)}(a^{(m)} - \bar{a}^{(l)})) \hat{\zeta}_p \exp(i\alpha_p x), \end{aligned}$$

c.f. (7). The Neumann condition, (14b), together with the formula (15) provides the equations

$$\begin{aligned}\psi^{(m)}(x) = \sum_{p=-\infty}^{\infty} \Big\{ & (-i\beta_p^{(m-1)}) d_p^{(m-1)} \exp(-i\beta_p^{(m-1)}(a^{(m)} - \bar{a}^{(m-1)})) \\ & + (i\beta_p^{(m-1)}) u_p^{(m-1)} \exp(i\beta_p^{(m-1)}(a^{(m)} - \bar{a}^{(m-1)})) \\ & + (i\beta_p^{(m)}) d_p^{(m)} \exp(-i\beta_p^{(m)}(a^{(m)} - \bar{a}^{(m)})) \\ & - (i\beta_p^{(m)}) u_p^{(m)} \exp(i\beta_p^{(m)}(a^{(m)} - \bar{a}^{(m)})) \Big\} \exp(i\alpha_p x),\end{aligned}$$

which can be alternatively expressed as

$$\psi^{(m)} = -B^{(m-1)} D^{(m,m-1)} d^{(m-1)} + B^{(m-1)} U^{(m,m-1)} u^{(m-1)} + B^{(m)} D^{(m,m)} d^{(m)} - B^{(m)} U^{(m,m)} u^{(m)}, \tag{17}$$

where we define the order–one Fourier multipliers, c.f. (8):

$$B^{(m)}[\zeta] := \sum_{p=-\infty}^{\infty} (i\beta_p^{(m)}) \hat{\zeta}_p \exp(i\alpha_p x).$$

Thus, we have the following system of linear equations to solve:

$$\mathcal{A}\vec{z} = \vec{r} \tag{18}$$

where

$$\begin{aligned} \vec{z} &:= (u^{(0)}, d^{(1)}, u^{(1)}, \dots, d^{(M-1)}, u^{(M-1)}, d^{(M)})^T, \\ \vec{r} &:= (\xi^{(1)}, \psi^{(1)}, \xi^{(2)}, \psi^{(2)}, \dots, \xi^{(M)}, \psi^{(M)})^T, \end{aligned}$$

and

$$\mathcal{A} := \begin{pmatrix} U_{1,0} & -D_{1,1} & -U_{1,1} & 0 & 0 & 0 \\ B_0 U_{1,0} & B_1 D_{1,1} & -B_1 U_{1,1} & 0 & 0 & 0 \\ 0 & D_{2,1} & U_{2,1} & -D_{2,2} & -U_{2,2} & 0 \\ 0 & -B_1 D_{2,1} & B_1 U_{2,1} & B_2 D_{2,2} & -B_2 U_{2,2} & 0 \\ \vdots & & & & & \vdots \\ 0 & 0 & 0 & D_{M,M-1} & U_{M,M-1} & -D_{M,M} \\ 0 & 0 & 0 & -B_{M-1} D_{M,M-1} & B_{M-1} U_{M,M-1} & B_M D_{M,M} \end{pmatrix}.$$

Of course all of these operators are diagonalized by the Fourier transform so we can solve, wavenumber–by–wavenumber, the systems

$$\mathcal{A}_p \vec{z}_p = \vec{r}_p \tag{19}$$

where

$$\begin{aligned} \vec{z}_p &:= (u_p^{(0)}, d_p^{(1)}, u_p^{(1)}, \dots, d_p^{(M-1)}, u_p^{(M-1)}, d_p^{(M)})^T, \\ \vec{r}_p &:= (\hat{\xi}_p^{(1)}, \hat{\psi}_p^{(1)}, \hat{\xi}_p^{(2)}, \hat{\psi}_p^{(2)}, \dots, \hat{\xi}_p^{(M)}, \hat{\psi}_p^{(M)})^T, \end{aligned}$$

and $\mathcal{A}_p$ is penta–diagonal:

$$\begin{aligned} (\mathcal{A}_p)_{2m-1,2m-2} &= (D_{m,m-1})_p = \exp(-i\beta_p^{(m-1)}(a^{(m)} - \bar{a}^{(m-1)})) \\ (\mathcal{A}_p)_{2m-1,2m-1} &= (U_{m,m-1})_p = \exp(i\beta_p^{(m-1)}(a^{(m)} - \bar{a}^{(m-1)})) \\ (\mathcal{A}_p)_{2m-1,2m} &= -(D_{m,m})_p = -\exp(-i\beta_p^{(m)}(a^{(m)} - \bar{a}^{(m)})) \\ (\mathcal{A}_p)_{2m-1,2m+1} &= -(U_{m,m})_p = -\exp(i\beta_p^{(m)}(a^{(m)} - \bar{a}^{(m)})) \\ (\mathcal{A}_p)_{2m,2m-2} &= -(B_{m-1}D_{m,m-1})_p = -(i\beta_p^{(m-1)})\exp(-i\beta_p^{(m-1)}(a^{(m)} - \bar{a}^{(m-1)})) \\ (\mathcal{A}_p)_{2m,2m-1} &= (B_{m-1}U_{m,m-1})_p = (i\beta_p^{(m-1)})\exp(i\beta_p^{(m-1)}(a^{(m)} - \bar{a}^{(m-1)})) \\ (\mathcal{A}_p)_{2m,2m} &= (B_m D_{m,m})_p = (i\beta_p^{(m)})\exp(-i\beta_p^{(m)}(a^{(m)} - \bar{a}^{(m)})) \\ (\mathcal{A}_p)_{2m,2m+1} &= -(B_m U_{m,m})_p = -(i\beta_p^{(m)})\exp(i\beta_p^{(m)}(a^{(m)} - \bar{a}^{(m)})), \end{aligned}$$

for $1 \leq m \leq M$; formulas which produce indices outside the range $1 \leq m \leq M$ (i.e. $(\mathcal{A}_p)_{1,0}$ and $(\mathcal{A}_p)_{M,M+1}$) are ignored. Since the system (18) is penta–diagonal it can be solved quickly (in time $\mathcal{O}(M)$) using standard techniques. This is the crucial observation which enables our accelerated method for couplers with non–trivial interface shapes.

3.2 Non–Trivial Interfaces

To address the case of non–trivial interfaces we can again use the representation (15) together with $d_p^{(0)} = u_p^{(M)} \equiv 0$. The Dirichlet and Neumann conditions remain (16) and (17), respectively, however we must now understand the operators $D^{(m,l)}$ and $U^{(m,l)}$ as $g^{(m)}$ dependent:

$$\begin{aligned} D^{(m,l)}(g^{(m)})[\zeta] &:= \sum_{p=-\infty}^{\infty} \exp(-i\beta_p^{(l)}(a^{(m)} + g^{(m)} - \bar{a}^{(l)}))\hat{\zeta}_p \exp(i\alpha_p x) \\ U^{(m,l)}(g^{(m)})[\zeta] &:= \sum_{p=-\infty}^{\infty} \exp(i\beta_p^{(l)}(a^{(m)} + g^{(m)} - \bar{a}^{(l)}))\hat{\zeta}_p \exp(i\alpha_p x). \end{aligned}$$

Following our previous developments, we pursue the Field Expansions (FE) method [5] beginning with the assumption that the interfaces $g^{(m)}$ are deviations of the trivial interface case, and that these deviations can be parametrized by the single variable ε, i.e. $g^{(m)}(x) = \varepsilon f^{(m)}(x)$. A generalization of the work of Nicholls & Reitich [25] will show that the fields $v^{(m)}$ depend analytically upon ε so that the expansions

$$\begin{aligned} v^{(m)} &= v^{(m)}(x, y; \varepsilon) \\ &= \sum_{p=-\infty}^{\infty} d_p^{(m)}(\varepsilon) \exp(i(\alpha_p x - \beta_p^{(m)}(y - \bar{a}^{(m)}))) + u_p^{(m)}(\varepsilon) \exp(i(\alpha_p x + \beta_p^{(m)}(y - \bar{a}^{(m)}))) \\ &= \sum_{p=-\infty}^{\infty} \sum_{n=0}^{\infty} \left\{ d_{p,n}^{(m)} \exp(i(\alpha_p x - \beta_p^{(m)}(y - \bar{a}^{(m)}))) + u_{p,n}^{(m)} \exp(i(\alpha_p x + \beta_p^{(m)}(y - \bar{a}^{(m)}))) \right\} \varepsilon^n \end{aligned} \tag{20}$$

can be rigorously justified provided that the $f^{(m)}$ are sufficiently small and smooth. To find the coefficients $d_{p,n}^{(m)}$ and $u_{p,n}^{(m)}$ we use the conditions (16) and (17) with the dependence of ε emphasized:

$$\xi^{(m)} = D^{(m,m-1)}(\varepsilon) d^{(m-1)}(\varepsilon) + U^{(m,m-1)}(\varepsilon) u^{(m-1)}(\varepsilon) - D^{(m,m)}(\varepsilon) d^{(m)}(\varepsilon) - U^{(m,m)}(\varepsilon) u^{(m)}(\varepsilon), \tag{21}$$

and

$$\begin{aligned} \psi^{(m)} = -B^{(m-1)} D^{(m,m-1)}(\varepsilon) d^{(m-1)}(\varepsilon) + B^{(m-1)} U^{(m,m-1)}(\varepsilon) u^{(m-1)}(\varepsilon) \\ + B^{(m)} D^{(m,m)}(\varepsilon) d^{(m)}(\varepsilon) - B^{(m)} U^{(m,m)}(\varepsilon) u^{(m)}(\varepsilon). \end{aligned} \tag{22}$$

To use these we need the Taylor expansions

$$D^{(m,l)}(\varepsilon f^{(m)}) = \sum_{n=0}^{\infty} D_n^{(m,l)}(f^{(m)}) \varepsilon^n, \quad U^{(m,l)}(\varepsilon f^{(m)}) = \sum_{n=0}^{\infty} U_n^{(m,l)}(f^{(m)}) \varepsilon^n,$$

where $D_0^{(m,l)} = D^{(m,l)}(0)$, $U_0^{(m,l)} = U^{(m,l)}(0)$,

$$D_n^{(m,l)}(f^{(m)})[\zeta] = F_n^{(m)} (-B^{(l)})^n D_0^{(m,l)} \zeta, \tag{23a}$$

$$U_n^{(m,l)}(f^{(m)})[\zeta] = F_n^{(m)} (B^{(l)})^n U_0^{(m,l)} \zeta, \tag{23b}$$

and $F_n^{(m)} := ((f^{(m)})^n)/n!$. With these we can realize the following recursions from (21) & (22): At order zero we have

$$D_0^{(m,m-1)} d_0^{(m-1)} + U_0^{(m,m-1)} u_0^{(m-1)} - D_0^{(m,m)} d_0^{(m)} - U_0^{(m,m)} u_0^{(m)} = \xi^{(m)} \tag{24a}$$

$$\begin{aligned} -B^{(m-1)} D_0^{(m,m-1)} d_0^{(m-1)} + B^{(m-1)} U_0^{(m,m-1)} u_0^{(m-1)} + B^{(m)} D_0^{(m,m)} d_0^{(m)} \\ -B^{(m)} U_0^{(m,m)} u_0^{(m)} = \psi^{(m)}, \end{aligned} \tag{24b}$$

which, of course, is simply (16) & (17) and we can solve this system, for each wavenumber, in linear time in M. For $n > 0$ we obtain

$$D_0^{(m,m-1)} d_n^{(m-1)} + U_0^{(m,m-1)} u_n^{(m-1)} - D_0^{(m,m)} d_n^{(m)} - U_0^{(m,m)} u_n^{(m)} = Q_n^{(m)} \tag{25a}$$

$$\begin{aligned} - B^{(m-1)} D_0^{(m,m-1)} d_n^{(m-1)} + B^{(m-1)} U_0^{(m,m-1)} u_n^{(m-1)} \\ + B^{(m)} D_0^{(m,m)} d_n^{(m)} - B^{(m)} U_0^{(m,m)} u_n^{(m)} = T_n^{(m)}, \end{aligned} \tag{25b}$$

where

$$Q_n^{(m)} := -\left\{ \sum_{l=0}^{n-1} D_{n-l}^{(m,m-1)} d_l^{(m-1)} + U_{n-l}^{(m,m-1)} u_l^{(m-1)} - D_{n-l}^{(m,m)} d_l^{(m)} - U_{n-l}^{(m,m)} u_l^{(m)} \right\} \tag{26a}$$

$$T_n^{(m)} := -\left\{ \sum_{l=0}^{n-1} -B^{(m-1)} D_{n-l}^{(m,m-1)} d_l^{(m-1)} + B^{(m-1)} U_{n-l}^{(m,m-1)} u_l^{(m-1)} \right.$$
$$\left. + B^{(m)} D_{n-l}^{(m,m)} d_l^{(m)} - B^{(m)} U_{n-l}^{(m,m)} u_l^{(m)} \right\} \tag{26b}$$

are known from the solution at previous orders. Using the calculation above in (23b) we can simplify the terms in (26):

$$Q_n^{(m)} = -\left\{ \sum_{l=0}^{n-1} F_{n-l}^{(m)} (-B^{(m-1)})^{n-l} D_0^{(m,m-1)} d_l^{(m-1)} + F_{n-l}^{(m)} (B^{(m-1)})^{n-l} U_0^{(m,m-1)} u_l^{(m-1)} \right.$$
$$\left. - F_{n-l}^{(m)} (-B^{(m)})^{n-l} D_0^{(m,m)} d_l^{(m)} - F_{n-l}^{(m)} (B^{(m)})^{n-l} U_0^{(m,m)} u_l^{(m)} \right\} \tag{27a}$$

$$T_n^{(m)} = -\left\{ \sum_{l=0}^{n-1} F_{n-l}^{(m)} (-B^{(m-1)})^{n-l+1} D_0^{(m,m-1)} d_l^{(m-1)} + F_{n-l}^{(m)} (B^{(m-1)})^{n-l+1} U_0^{(m,m-1)} u_l^{(m-1)} \right.$$
$$\left. - F_{n-l}^{(m)} (-B^{(m)})^{n-l+1} D_0^{(m,m)} d_l^{(m)} - F_{n-l}^{(m)} (B^{(m)})^{n-l+1} U_0^{(m,m)} u_l^{(m)} \right\}. \tag{27b}$$

Our key observation is that (25) is simply (18) with the right hand side replaced by

$$\vec{R}_n := (Q_n^{(1)}, T_n^{(1)}, Q_n^{(2)}, T_n^{(2)}, \dots, Q_n^{(M)}, T_n^{(M)})^T,$$

and can therefore be solved rapidly via standard techniques. In fact, a quick count of operations yields a work estimate of $\mathcal{O}(MN^2 N_x \log(N_x))$ if we truncate our Fourier–Taylor series $\{d_{p,n}^{(m)}, u_{p,n}^{(m)}\}$ after N_x modes and N orders. More precisely, at every Taylor order $0 \le n \le N$, and every wavenumber $-N_x/2 \le p \le N_x/2 - 1$, we solve a linear system of size M in linear time. To *form* the right hand sides of the linear system requires fast convolutions (via the FFT algorithm in time $\mathcal{O}(N_x \log(N_x))$), and a sum of length n (over indices $0 \le l \le n-1$).

This is to be contrasted with the work of Wilcox, Dinesen, & Hesthaven [32] who solve these layer problems sequentially using the two–layer solver of Bruno & Reitich [5]. For instance, in the three–layer case outlined in § 2, incident radiation from below results in a field scattered by the lowest layer at $y = \bar{h} + h(x)$ which is partially reflected downward and partially transmitted upwards. Wilcox *et al* compute these at the interface $y = \bar{h} + h(x)$ with a two–layer solver, but now must account for the fact that the transmitted field will interact with the layer at $y = \bar{g} + g(x)$ producing a scattered field transmitting further up the structure *and* a reflected field which travels back to $y = \bar{h} + h(x)$. This transmitted/reflected pair is computed in the second "bounce," but this procedure continues *ad infinitum* (albeit with decreasing amplitude in the inner part of the structure at every bounce). So, to compare with the cost of our new approach, that of Wilcox *et al* is $\mathcal{O}(BN^2 N_x \log(N_x))$ where B is the number of bounces required to reach a certain error tolerance. These authors report values of B in the range of 500–1000 for configurations with $M = 2$ interfaces, clearly disadvantaged with respect to our new approach.

4 Numerical Results

In this section we display how the algorithms we have described can be used in multi–layer simulations. In brief, the method discussed above can be summarized as a Fourier Collocation [11]/Taylor method [23] enhanced by Padé summation techniques [1]. In more detail, we approximate the fields $v^{(m)}$, c.f. (20), by

$$v^{(m,N_x,N)} = \sum_{p=-N_x/2}^{N_x/2-1} \sum_{n=0}^{N} \left\{ d_{p,n}^{(m)} \exp(i(\alpha_p x - \beta_p^{(m)}(y - \bar{a}^{(m)}))) + u_{p,n}^{(m)} \exp(i(\alpha_p x + \beta_p^{(m)}(y - \bar{a}^{(m)}))) \right\} \varepsilon^n, \tag{28}$$

which are then inserted into (25). At this point the only considerations are how the convolution products present in the right hand sides, $\{Q_n, R_n\}$ c.f. (26), are to be computed, and how the sum in ε is to be formed. For the former we utilize the Discrete Fourier Transform accelerated by the Fast Fourier Transform algorithm [11], and for the latter we approximate the truncated order N Taylor series by its $N/2$–$N/2$ Padé approximant.

We now present results of two numerical experiments featuring three– and five–layer structures. In both of these experiments we have chosen $d = 2\pi$ periodic interfaces with $\alpha = 0.1$. In the three–layer case we have selected

$$\begin{gathered} \beta_u = 1.1, \quad \beta_v = 2.2, \quad \beta_w = 3.3, \\ \bar{g} = -1, \quad g(x) = \varepsilon\cos(x), \quad \bar{h} = 1, \quad h(x) = \varepsilon\sin(2x), \end{gathered} \tag{29}$$

and $\varepsilon = 0.1$. For numerical parameters we selected $N_x = 128$ and $N = 24$. To verify the accuracy of our simulations we consider the "energy defect" in our solution. For a lossless structure like the ones considered in this paper, it is known that the total energy is conserved [27]. This principal can be stated precisely in terms of the efficiencies

$$e_p^{(0)} := \frac{\left|u_p^{(0)}\right|^2 \beta_p^{(0)}}{\beta} \qquad p \in U^{(0)} = \left\{ p \mid \alpha_p^2 < (k^{(0)})^2 \right\}$$

$$e_p^{(M)} := \frac{\left|d_p^{(M)}\right|^2 \beta_p^{(M)}}{\beta} \qquad p \in D^{(M)} = \left\{ p \mid \alpha_p^2 < (k^{(M)})^2 \right\},$$

which characterize the "outgoing energy fraction" propagating away from the structure upward and downward, respectively. Conservation of energy is now stated precisely as

$$\sum_{p \in U^{(0)}} e_p^{(0)} + \sum_{p \in D^{(M)}} e_p^{(M)} = 1,$$

and we can use as a diagnostic of convergence the "energy defect":

$$\delta := 1 - \sum_{p \in U^{(0)}} e_p^{(0)} + \sum_{p \in D^{(M)}} e_p^{(M)}. \tag{30}$$

In Table 1 we display results of this energy defect, δ, as N, the number of terms retained in the Taylor series is increased. Clearly, the convergence is exponential (down to machine zero) as we would expect. In Figure 2 we plot the real (left) and imaginary (right) parts of the scattered acoustic field with the layer interfaces superimposed with solid lines. In Figure 3 we display the real (left) and imaginary (right) parts of the *total* field for the same experiment.

In the five–layer case we chose

$$\begin{gathered} \beta^{(m)} = (1.1, 2.2, 3.3, 4.4, 5.5), \quad a^{(m)} = (1.5, 0.5, -0.5, -1.5), \\ g^{(m)} = (\cos(x), \sin(2x), \cos(3x), \sin(4x)), \end{gathered} \tag{31}$$

and $\varepsilon = 0.1$. Again, for numerical parameters we selected $N_x = 128$ and $N = 24$. In Table 2 we display results of this energy defect, δ, as N, the number of terms retained in the Taylor series is increased. Again,

Table 1: Energy defect (δ) versus number of Taylor series terms retained, c.f. (28), in a simulation of scattering by a three–layer structure. Physical parameters are reported in (29), while the numerical parameters were $N_x = 128$ and $N_{max} = 24$.

N	Energy Defect (δ)
0	0.00547926
2	0.00206438
4	-2.27676×10^{-5}
6	-1.52311×10^{-7}
8	3.93408×10^{-8}
10	-3.12122×10^{-9}
12	1.76252×10^{-10}
14	-7.7639×10^{-12}
16	2.60902×10^{-13}
18	-5.44009×10^{-15}
20	-3.33067×10^{-16}
22	0
24	0

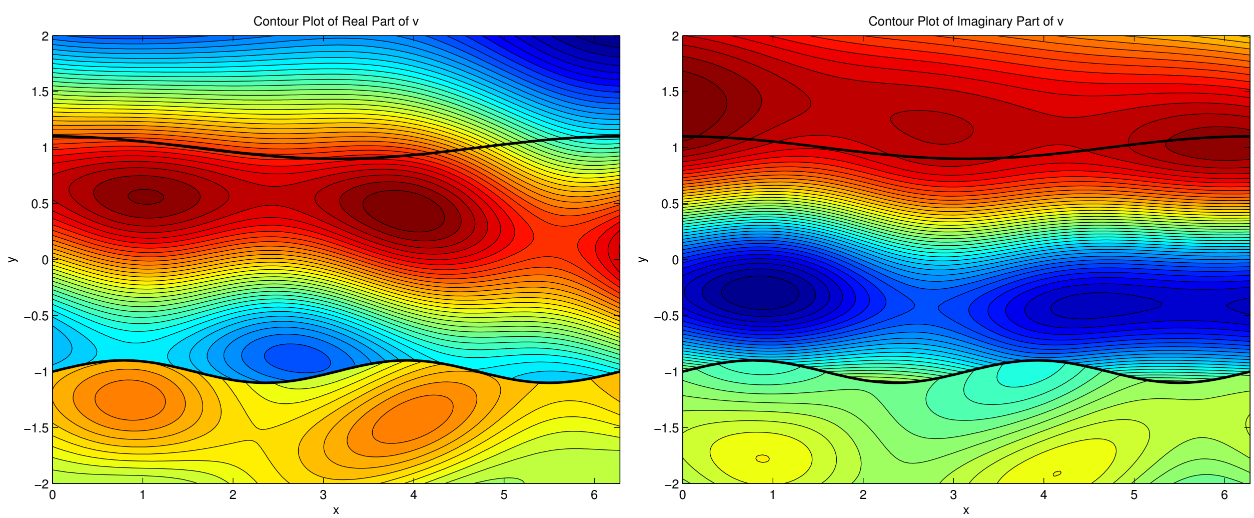

Figure 2: A plot of the scattered field (Left: Real part, Right: Imaginary part) in a simulation of scattering by a three–layer structure. Physical parameters are reported in (29), while the numerical parameters were $N_x = 128$ and $N = 24$.

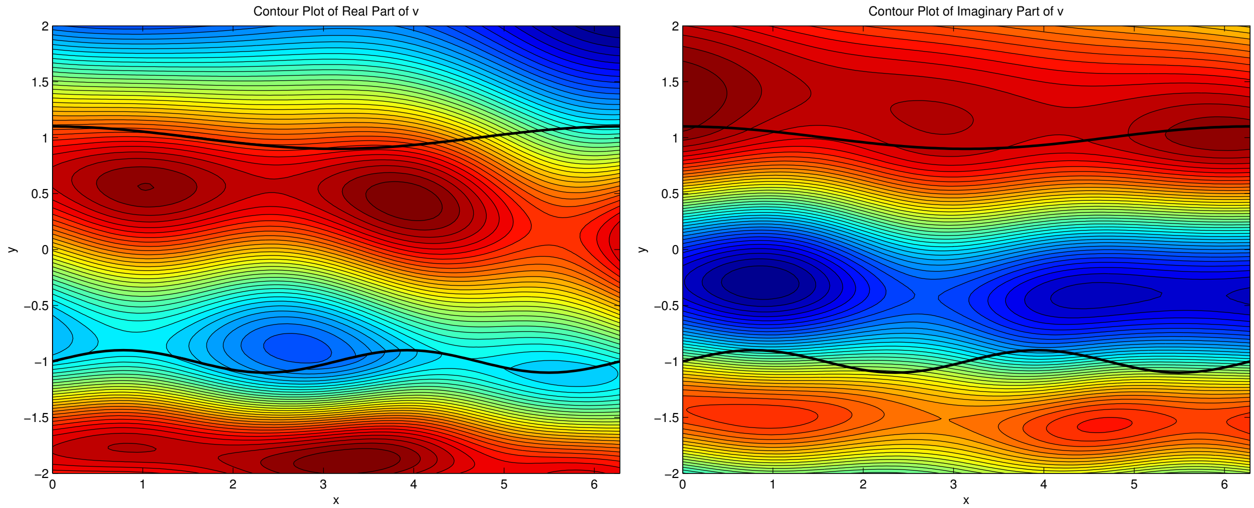

Figure 3: A plot of the total field (Left: Real part, Right: Imaginary part) in a simulation of scattering by a three–layer structure. Physical parameters are reported in (29), while the numerical parameters were $N_x = 128$ and $N = 24$.

Table 2: Energy defect (δ) versus number of Taylor series terms retained, c.f. (28), in a simulation of scattering by a five–layer structure. Physical parameters are reported in (31), while the numerical parameters were $N_x = 128$ and $N_{max} = 24$.

N	Energy Defect (δ)
0	0.0197169
2	0.0171099
4	-0.000155799
6	-4.50847×10^{-5}
8	3.0206×10^{-6}
10	-8.05347×10^{-8}
12	2.20133×10^{-9}
14	-5.54635×10^{-10}
16	7.60854×10^{-11}
18	-5.36948×10^{-12}
20	1.56319×10^{-13}
22	8.21565×10^{-15}
24	2.17604×10^{-14}

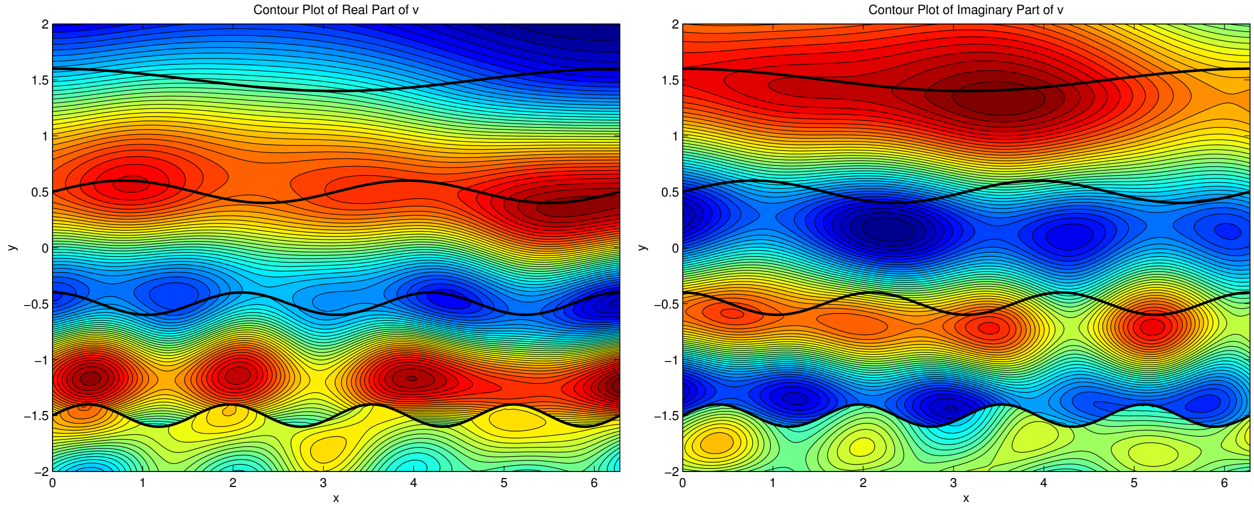

Figure 4: A plot of the scattered field (Left: Real part, Right: Imaginary part) in a simulation of scattering by a five–layer structure. Physical parameters are reported in (31), while the numerical parameters were $N_x = 128$ and $N = 24$.

we note exponential convergence (down to machine zero) as expected. In Figure 4 we depict the real (left) and imaginary (right) parts of the scattered acoustic field with the layer interfaces superimposed with solid lines.

To conclude, we present results of some preliminary numerical simulations of a point–source disturbance within the lowest layer meant to model a subterranean earthquake. As we saw in (2g), the incident radiation can be quite general and our point–source model is no exception provided that we consider a *periodic* family of point sources, which is quite natural given the periodic nature of our interfaces. With this specification, we recall that such a function can be defined with the upward propagating, periodized free–space Green's function [27]

$$G_{qp}(x,y) = -\frac{i}{4} \sum_{p=-\infty}^{\infty} e^{i\alpha p d} H_0^{(1)} \left(k\sqrt{(x-pd)^2 + y^2} \right),$$

where $H_0^{(1)}$ is the zeroth–order Hankel function of the first kind. If the singularity is located at (x_0, y_0) then the point–source is given by

$$w_{ps}(x,y) := G_{qp}(x - x_0, y - y_0).$$

For utilization in our recursions it is more convenient to use the *spectral representation* [27]

$$G_{qp}(x,y) = \frac{1}{2id} \sum_{p=-\infty}^{\infty} \frac{e^{i(\alpha_p x + \beta_p |y|)}}{\beta_p},$$

and, again, $w_{ps}(x,y) := G_{qp}(x - x_0, y - y_0)$. Setting $w_i = w_{ps}$, $(x_0, y_0) = (d/2, -20)$ and $\alpha = 0$ (so that the point sources are *periodic* rather than quasiperiodic) we can now test the capabilities of our method in the three–layer configuration outlined above; c.f. (29) with $\varepsilon = 0.1$. In Table 3 we report computations of the scattering efficiencies e_0 and e_{-2} in the upper layer as the perturbation order N is increased. As we have seen in all of the simulations above, a rapid and stable convergence of the efficiency is displayed as the perturbation order is increased resulting in full double precision accuracy by $N = 24$.

Table 3: Efficiencies versus number of Taylor series terms retained, c.f. (28), in a simulation of point–source scattering by a three–layer structure. Physical parameters are reported in (29), while the numerical parameters were $N_x = 128$ and $N_{max} = 24$.

N	e_0	e_{-2}
0	$2.638809126959936 \times 10^{-5}$	0.0005213256160486521
2	$4.317263372822617 \times 10^{-5}$	0.0006943499382756026
4	$4.063250064761511 \times 10^{-5}$	0.0006894970545861178
6	$4.075330989714637 \times 10^{-5}$	0.0006894225965224039
8	$4.075037414093768 \times 10^{-5}$	0.0006894312866295445
10	$4.075036372657268 \times 10^{-5}$	0.0006894309333885411
12	$4.075036820779545 \times 10^{-5}$	0.0006894309404349986
14	$4.075036798603324 \times 10^{-5}$	0.0006894309405442724
16	$4.075036799146814 \times 10^{-5}$	0.0006894309405292778
18	$4.075036799148951 \times 10^{-5}$	0.0006894309405298982
20	$4.075036799148102 \times 10^{-5}$	0.0006894309405298865
22	$4.075036799148142 \times 10^{-5}$	0.0006894309405298864
24	$4.075036799148141 \times 10^{-5}$	0.0006894309405298864

Acknowledgments

DPN gratefully acknowledges support from the National Science Foundation through grant No. DMS–0810958, and the Department of Energy under Award No. DE–SC0001549. AM acknowledges the support of the Earth Resources Laboratory Founding Members Consortium.

Disclaimer: This report was prepared as an account of work sponsored by an agency of the United States Government. Neither the United States Government nor any agency thereof, nor any of their employees, make any warranty, express or implied, or assumes any legal liability or responsibility for the accuracy, completeness, or usefulness of any information, apparatus, product, or process disclosed, or represents that its use would not infringe privately owned rights. Reference herein to any specific commercial product, process, or service by trade name, trademark, manufacturer, or otherwise does not necessarily constitute or imply its endorsement, recommendation, or favoring by the United States Government or any agency thereof. The views and opinions of authors expressed herein do not necessarily state or reflect those of the United States Government or any agency thereof.

References

[1] George A. Baker, Jr. and Peter Graves-Morris. *Padé approximants*. Cambridge University Press, Cambridge, second edition, 1996.

[2] Florian Bleibinhaus and Stéphane Rondenay. Effects of surface scattering in full-waveform inversion. *Geophysics*, 74(6):WCC69–WCC77, 2009.

[3] M Bouchon. A review of the discrete wavenumber method. *Pure appl. geophys.*, 160(3):445–465, 2003.

[4] Oscar P. Bruno and Fernando Reitich. Solution of a boundary value problem for the Helmholtz equation via variation of the boundary into the complex domain. *Proc. Roy. Soc. Edinburgh Sect. A*, 122(3-4):317–340, 1992.

[5] Oscar P. Bruno and Fernando Reitich. Numerical solution of diffraction problems: A method of variation of boundaries. *J. Opt. Soc. Am. A*, 10(6):1168–1175, 1993.

[6] Oscar P. Bruno and Fernando Reitich. Numerical solution of diffraction problems: A method of variation of boundaries. II. Finitely conducting gratings, Padé approximants, and singularities. *J. Opt. Soc. Am. A*, 10(11):2307–2316, 1993.

[7] Oscar P. Bruno and Fernando Reitich. Numerical solution of diffraction problems: A method of variation of boundaries. III. Doubly periodic gratings. *J. Opt. Soc. Am. A*, 10(12):2551–2562, 1993.

[8] P. G. Dinesen and J. S. Hesthaven. Fast and accurate modeling of waveguide grating couplers. *J. Opt. Soc. Am. A*, 17(9):1565–1572, 2000.

[9] P. G. Dinesen and J. S. Hesthaven. Fast and accurate modeling of waveguide grating couplers. ii. the three-dimensional vectorial case. *J. Opt. Soc. Am. A*, 18(11):2876–2885, 2001.

[10] L Geli, PY Bard, and B Jullien. The effect of topography on earthquake ground motion: a review and new results. *Bulletin of the Seismological Society of America*, 78(1):42, 1988.

[11] David Gottlieb and Steven A. Orszag. *Numerical analysis of spectral methods: theory and applications*. Society for Industrial and Applied Mathematics, Philadelphia, Pa., 1977. CBMS-NSF Regional Conference Series in Applied Mathematics, No. 26.

[12] L. Greengard and V. Rokhlin. A fast algorithm for particle simulations. *J. Comput. Phys.*, 73(2):325–348, 1987.

[13] K. Koketsu, H. Fujiwara, and Y. Ikegami. Finite-element simulation of seismic ground motion with a voxel mesh. *Journal Pure and Applied Geophysics*, 161(11-12), 2004.

[14] D. Komatitsch and J. Tromp. Spectral-element simulations of global seismic wave propagation-I. Validation. *Geophysical Journal International*, 149(2):390–412, 2002.

[15] D. Komatitsch and J. Tromp. Spectral-element simulations of global seismic wave propagation-II. 3-D models, oceans, rotation, and self-gravitation. *Geophysical Journal International*, 150(1):303–318, 2002.

[16] D. Michael Milder. An improved formalism for rough-surface scattering of acoustic and electromagnetic waves. In *Proceedings of SPIE - The International Society for Optical Engineering (San Diego, 1991)*, volume 1558, pages 213–221. Int. Soc. for Optical Engineering, Bellingham, WA, 1991.

[17] D. Michael Milder. An improved formalism for wave scattering from rough surfaces. *J. Acoust. Soc. Am.*, 89(2):529–541, 1991.

[18] D. Michael Milder. An improved formalism for electromagnetic scattering from a perfectly conducting rough surface. *Radio Science*, 31(6):1369–1376, 1996.

[19] D. Michael Milder. Role of the admittance operator in rough-surface scattering. *J. Acoust. Soc. Am.*, 100(2):759–768, 1996.

[20] D. Michael Milder and H. Thomas Sharp. Efficient computation of rough surface scattering. In *Mathematical and numerical aspects of wave propagation phenomena (Strasbourg, 1991)*, pages 314–322. SIAM, Philadelphia, PA, 1991.

[21] D. Michael Milder and H. Thomas Sharp. An improved formalism for rough surface scattering. ii: Numerical trials in three dimensions. *J. Acoust. Soc. Am.*, 91(5):2620–2626, 1992.

[22] P Moczo, JOA Robertsson, and L Eisner. The finite-difference time-domain method for modeling of seismic wave propagation. *Advances in Geophysics*, 48:421, 2007.

[23] David P. Nicholls and Fernando Reitich. Stability of high-order perturbative methods for the computation of Dirichlet-Neumann operators. *J. Comput. Phys.*, 170(1):276–298, 2001.

[24] David P. Nicholls and Fernando Reitich. Shape deformations in rough surface scattering: Cancellations, conditioning, and convergence. *J. Opt. Soc. Am. A*, 21(4):590–605, 2004.

[25] David P. Nicholls and Fernando Reitich. Shape deformations in rough surface scattering: Improved algorithms. *J. Opt. Soc. Am. A*, 21(4):606–621, 2004.

[26] David P. Nicholls and Fernando Reitich. Boundary perturbation methods for high–frequency acoustic scattering: Shallow periodic gratings. *submitted*, 2007.

[27] Roger Petit, editor. *Electromagnetic theory of gratings*. Springer-Verlag, Berlin, 1980.

[28] R. Gerhard Pratt. Frequency-domain elastic wave modeling by finite differences: A tool for crosshole seismic imaging. *Geophysics*, 55(5):626–632, 1990.

[29] F. J. Sanchez-Sesma, V. J. Palencia, and F. Luzon. Estimation of local site effects during earthquakes: An overview. In V. K. Gupta, editor, *FROM SEISMIC SOURCE TO STRUCTURAL RESPONSE:CONTRIBUTIONS OF PROFESSOR MIHAILO D. TRIFUNAC*, pages 44–70. University of Southern California, Department of Civil Engineering, 2004.

[30] FJ Sanchez-Sesma and E Perez-Rocha. Diffraction of elastic waves by three-dimensional surface irregularities. part ii. *Bulletin of the Seismological Society of America*, 79(1):101, 1989.

[31] J Virieux and S Operto. An overview of full-waveform inversion in exploration geophysics. *link.aip.org*, Jan 2009.

[32] L. C. Wilcox, P. G. Dinesen, and J. S. Hesthaven. Fast and accurate boundary variation method for multilayered diffraction optics. *J. Opt. Soc. Am. A*, 21(5):757–769, 2004.

[33] O. C. Zienkiewicz. *The Finite Element Method in Engineering Science, 3rd ed.* McGraw-Hill, New York, 1977.